

Spontaneous Formation of Nucleic Acid-based Nanoparticles Is Responsible for High Interferon- α Induction by CpG-A in Plasmacytoid Dendritic Cells*

Received for publication, September 21, 2004, and in revised form, December 3, 2004
Published, JBC Papers in Press, December 8, 2004, DOI 10.1074/jbc.M410868200

Miren Kerkmann^{‡§}, Lilian T. Costa[¶], Christine Richter[‡], Simon Rothenfusser[‡], Julia Battiany[‡], Veit Hornung[‡], Judith Johnson^{**}, Steffen Englert^{‡‡}, Thomas Ketterer^{§§}, Wolfgang Heckl[¶], Stefan Thalhammer[¶], Stefan Endres[‡], and Gunther Hartmann^{‡¶¶}

From the [‡]Department of Internal Medicine, Division of Clinical Pharmacology, Ludwig-Maximilians-University of Munich, 80336 Muenchen, Germany, [¶]Department of Geo- and Environment Sciences, Ludwig-Maximilians-University of Munich, 80333 Muenchen, Germany, ^{**}Institute of Immunology, Ludwig-Maximilians-University of Munich, 80336 Muenchen, Germany, ^{§§}CureVac GmbH, 72076 Tuebingen, Germany, and ^{‡‡}Research Center for Nucleic Acid and Peptide Chemistry, University of Tuebingen, 72076 Tuebingen, Germany

Plasmacytoid dendritic cells (PDC) represent a highly specialized immune cell subset that produces large quantities of the anti-viral cytokines type I interferons (IFN- α and IFN- β) upon viral infection. PDC employ a member of the family of toll-like receptors, TLR9, to detect CpG motifs (unmethylated CG dinucleotides in certain base context) present in viral DNA. A certain group of CpG motif-containing oligodeoxynucleotides (CpG ODN), CpG-A, was the first synthetic stimulus available that induced large amounts of interferon- α (IFN- α) in PDC. However, the mechanism responsible for this activity remained elusive. CpG-A is characterized by a central palindrome and poly(G) at the 5' and 3' end. Here we demonstrate that CpG-A self-assembles to higher order tertiary structures via G-tetrad formation of their poly(G) motifs. Spontaneous G-tetrad formation of CpG-A required the palindrome sequence allowing structure formation in a physiological environment. Once formed, G-tetrad-linked structures were stable even under denaturing conditions. Atomic force microscopy revealed that the tertiary structures formed by CpG-A represent nucleic acid-based nanoparticles in the size range of viruses. Similarly sized preformed polystyrene nanoparticles loaded with a CpG ODN that is otherwise weak at inducing IFN- α (CpG-B) gained the potency of CpG-A to induce IFN- α . Higher ODN uptake in PDC was not responsible for the higher IFN- α -inducing activity of CpG-A or of CpG-B-coated nanoparticles as compared with CpG-B. Based on these results we propose a model in which the spatial configuration of CpG motifs as particle is responsible for the virus-like potency of CpG-A to induce IFN- α in PDC.

The induction of natural type I interferons (IFNs)¹ (anti-viral cytokines, IFN- α and IFN- β) *in vivo* may pave the way for improved therapies for viral infection such as chronic hepatitis or for malignancies. A particular immune cell subset, the so-called plasmacytoid dendritic cell (PDC), has been identified as the major type I interferon-producing cell upon viral infection (1, 2). Viruses for a long time have been the only stimuli to induce large amounts of IFN- α in PDC. Recently it became clear that certain members of the family of toll-like receptors (TLRs) are involved in the regulation of IFN- α synthesis in PDC. In general, TLRs (TLR1–TLR10) are specialized for the detection of conserved pathogen-associated molecules such as endotoxin (component of Gram-negative bacteria, detected by TLR4) leading to activation of the corresponding immune cell subset (3). The only two TLRs expressed in PDC are TLR7 and TLR9 (4–6). Consequently, PDC can be stimulated by the corresponding ligands for TLR7 and TLR9. Although DNA containing so-called CpG motifs (unmethylated CG dinucleotides with certain flanking bases, CpG-DNA) has been identified as a ligand for TLR9 early on (7), CpG motif containing synthetic oligodeoxynucleotides (CpG ODN) only induce large amounts of IFN- α in PDC when they fulfill certain sequence requirements (palindrome, two poly(G) ends, phosphorothioate-modified linkages at the 5' and 3' ends) in addition to the CpG motif; this group of CpG ODN is termed CpG-A (8, 9). The prototype sequence of CpG-A is ODN 2216 (8). ODN 2006 (10, 11), the sequence currently being tested in a number of clinical trials (ProMune, ODN 7909), belongs to the group of CpG-B. CpG-B are weak at inducing IFN- α but are more active than CpG-A to stimulate costimulatory molecules and proinflammatory cytokines and to promote survival and differentiation of PDC (5). The most recent group of CpG ODN is CpG-C, which induces intermediate levels of IFN- α in PDC and directly activates B cells (12–15).

Regulation of type I IFN production in PDC by the different classes of CpG ODN is not well understood. In studies with TLR9-deficient mice it has been demonstrated that both CpG-A and CpG-B depend on TLR9 (16). However, CpG-B shows much higher activity in TLR9-transfected cell lines than CpG-A.²

* This study was supported in part by a grant from the Bundesministerium für Bildung und Forschung (Biofuture 0311896), Deutsche Forschungsgemeinschaft Grants HA 2780/4-1 and SFB 571, Dr. Mildred Scheel Stiftung Grant 10-2074, and a grant from the Human Science Foundation of Japan (to G. H.). The costs of publication of this article were defrayed in part by the payment of page charges. This article must therefore be hereby marked "advertisement" in accordance with 18 U.S.C. Section 1734 solely to indicate this fact.

¶ This work is part of the dissertation of this author at the Ludwig-Maximilians-University of Munich.

¶ Financially supported by the Deutscher Akademischer Austauschdienst and Deutsche Forschungsgemeinschaft Sonderforschungsbe- reich 486.

¶¶ To whom correspondence should be addressed: Abteilung für Klinische Pharmakologie, Medizinische Klinik Innenstadt, Klinikum der Ludwig-Maximilians-Universität München, Ziemssenstrasse 1, 80336 München, Germany. Tel.: 49-89-5160-2331; Fax: 49-89-5160-4406; E-mail: ghartmann@lrz.uni-muenchen.de.

¹ The abbreviations used are: IFN, interferon; PDC, plasmacytoid dendritic cell(s); TLR, toll-like receptor; ODN, oligodeoxynucleotide(s); PBS, phosphate-buffered saline without calcium and magnesium; AFM, atomic force microscopy; TBE, Tris-borate-EDTA.

² S. Akira, personal communication.

TABLE I
Sequences of ODN used

Small letters, phosphorothioate linkage; capital letters, phosphodiester linkage 3' of the base; bold, CpG-dinucleotides; *m*, 7-deazaguanosine substitution.

Class	Name	Sequence 5' to 3'
CpG-B	ODN 2006	t cg t cg ttt tgt cg t ttt gtc g tt
CpG-B control	CpG-B GC	tgc tgc ttt tgt gct ttt gtg ctt
CpG-A	ODN 2216	ggG GGA CGA TCG TCg ggg gG
	ODN 1585	ggG GTC AAC G TT Gag ggg gG
CpG-A controls	CpG-A GC	ggG GGA GCA TGC TGc ggg gG
	CpG-A polyC	ccC CCA CGA TCG TCc ccc cC
	CpG-A mis	ggG GGT CGA ACG TCg ggg gG
	CpG-A deaza	ggmG GTC AAC G TT Gag ggmG gG
Tet 1.5		GGG GTT GGG G

Because TLR9 is required for both CpG-A and CpG-B, it is intriguing that ligation of the same receptor, TLR9, can elicit distinct responses in PDC.

ODNs with poly(G) motifs (at least four guanines) are known to self-associate via Hoogsteen base pairing into quadruplex structures, so-called G-tetrads (17–19). The formation and the stability of quadruplex ODNs depend on the sequence as well as on the concentrations of monovalent cations such as sodium and potassium in the ODN diluent (20, 21). It has been suggested that the formation of G-tetrad-stabilized structures is involved in immunoglobulin switch regions and in chromosomal telomeres, both of which contain guanosine-rich sequences (22, 23).

Here we demonstrate that the CpG-A ODN 2216 spontaneously and under physiological conditions forms nanoparticles via G-tetrads. Based on our results we propose a concept in which the palindrome sequence of CpG-A via duplex formation of two CpG-A molecules facilitates the generation of G-tetrads and in which the spatial configuration of CpG motifs as a nanoparticle is critical for the high IFN- α inducing activity characteristic for CpG-A.

MATERIALS AND METHODS

Media and Reagents—RPMI cell culture medium (PAA Laboratories, Linz, Austria) supplemented with 8% human serum (BioWhittaker, Walkersville, MD), 1.5 mM L-glutamine, 100 units/ml penicillin and 100 μ g/ml streptomycin (Sigma, Munich, Germany) was used throughout the studies. All compounds were purchased endotoxin-free. ODN were provided by Coley Pharmaceutical Group (Wellesley, MA) or purchased from Metabion (Martinsried, Germany). Sequences of the ODN used in this study are provided in Table I. No endotoxin could be detected in ODN preparations using the limulus amoebocyte lysate assay (BioWhittaker; lower detection limit 0.03 enzyme units/ml). ODN were used at a final concentration of 3 μ g/ml as established earlier (8). Acrylamide solution was from Bio-Rad. [³²P]ATP, 5' end labeling kit, and oligonucleotide sizing markers were purchased from Amersham Biosciences. PBS (phosphate-buffered saline without calcium and magnesium) was from PAA Laboratories (Linz, Austria). Chemicals were from Merck KGa (Darmstadt, Germany). Mica was purchased from Plano GmbH.

Gel Electrophoresis—ODN were radiolabeled at the 5' end with [³²P]ATP using the 5' end labeling kit according to the protocol provided by the manufacturer. Higher order structure formation of ODN in PBS was analyzed by gel electrophoresis. Non-denaturing gel electrophoresis: 20% polyacrylamide, 1 \times TBE; loading buffer: 20% sucrose, 1 \times TBE, 0.05% bromphenol blue (Sigma), 0.05% xylene cyanole (Sigma). The gel was run at a constant electric field of 8 V/cm; denaturing gel electrophoresis: 20% polyacrylamide, 1 \times TBE, 8 M urea; loading buffer: 80% formamide; 1 \times TBE; 0.05% bromphenol blue; 0.05% xylene cyanole. The gel was run at a constant electric field of 40 V/cm. For denaturing gel analysis an oligonucleotide sizing marker was labeled with [³²P]ATP. For the analysis of structure formation in different buffers and temperatures, 5'-digoxigenin-labeled ODN were purchased from Metabion (Martinsried, Germany). Immunological detection of digoxigenin-labeled ODN was performed by using the anti-digoxigenin-alkaline phosphatase and the digoxigenin Wash and Block buffer set (both from Roche Applied Sciences) according to the instructions provided by the manufacturer. Structure formation under the following buffers

were analyzed (22): buffer A, 143 mM NaCl, 4 mM KCl, 10 mM Tris-HCl, pH 7.25 (interstitial milieu); buffer B, 10 mM NaCl, 155 mM KCl, 10 mM Tris-HCl, pH 7.25 (intracellular milieu); buffer C, 150 mM NaCl, 10 mM KCl, 10 mM Tris-HCl, pH 7.25 (15:1 buffer). These analyses were performed using 16% polyacrylamide gels under non-denaturing conditions with 10 mM and 0.5 \times TBE. These gels were run for 30 min at 100 V followed by 3 h at 200 V.

Atomic Force Microscopy—ODN diluted in PBS without Ca²⁺ and Mg²⁺ (PAA Laboratories) were deposited on pretreated mica (25 mM MgCl₂ spin coating for 1 min), incubated for 5 min, washed with purified water, and dried under vacuum as described earlier (24). All images were performed using a Topometrix Explorer (Darmstadt, Germany) operating in dynamic mode at ambient conditions using cantilevers NSC11 (Ultrasharp) with a spring constant 3 N/m and a resonance frequency of \sim 45 kHz. The nominal tip radius was < 10.0 nm. Image analysis was performed using SPIP software (Lyngby, Denmark).

Isolation of Cells and Cell Culture—Buffy coats from 18- to 65-year-old healthy donors tested to be negative for human immunodeficiency virus, hepatitis B virus, and hepatitis C virus were provided by the blood bank of the University of Greifswald. Human peripheral blood mononuclear cells were prepared from buffy coats by Ficoll-Hypaque density gradient centrifugation (Biochrom) as described (25). PDC were isolated by magnetically activated cell sorting using the BDCA-4 dendritic cell isolation kit from Milteny Biotec (Bergisch-Gladbach, Germany). Briefly, PDC were labeled with anti-BDCA-4 antibody coupled to colloidal paramagnetic microbeads and passed through a magnetic separation column twice (LS and RS column, Milteny Biotec). The purity of isolated PDC (lineage-negative, MHC II-positive, and CD123-positive cells) was >90%. (Viability was >95% as determined by trypan blue exclusion). Isolated PDC (5 \times 10⁴ cells/well) or peripheral blood mononuclear cells (4 \times 10⁵ cells/well) were cultured in 96-well round-bottom plates in the presence of different stimuli as indicated. CpG ODN were used at a final concentration of 3 μ g/ml. Supernatants were collected after different periods of time for cytokine analysis.

Nanoparticle Preparation and Formation of Nanoparticle-ODN Conjugates—Polystyrene nanoparticles were prepared by batch polymerization under surfactant-free conditions as described by Fritz *et al.* (26). The cationic initiator AIBI was applied to induce positive surface charge. Additional steric stabilization was achieved by the addition of the nonionic surfactant poloxamer 338. The size of the nanospheres was determined by photon correlation spectroscopy using a photon correlation spectrometer Zetasizer 4 (Malvern Instruments, Malvern, UK) and amounts to 180 nm. Adsorption of CpG ODN to polystyrene nanoparticles was performed as described by Fritz *et al.* (26).

Flow Cytometry—Fluorescein isothiocyanate-labeled ODN were purchased from Metabion (Martinsried, Germany). For the analysis of ODN uptake PDC were incubated with fluorescein isothiocyanate-labeled ODN or fluorescein isothiocyanate-labeled ODN adsorbed to polystyrene nanoparticles (final concentration of ODN, 3 μ g/ml) at 37 °C. Surface binding of ODN was determined by incubation at 4 °C. After 1.5 h cells were washed twice and fluorescence intensity was measured by flow cytometry (FACSCalibur with two lasers, excitation at 488 and 635 nm wavelength, BD Biosciences). Dead cells were excluded from the analysis by morphologic criteria. Data were analyzed using Cell Quest software (BD Biosciences).

Detection of Cytokines—The IFN- α module set from Bender MedSystems (detection range 8–500 pg/ml) and the human TNF- α enzyme-linked immunosorbent assay (detection range, 8–500 pg/ml) from BD Pharmingen were used.

Statistical Analysis—Data are shown as means \pm S.E. Statistical

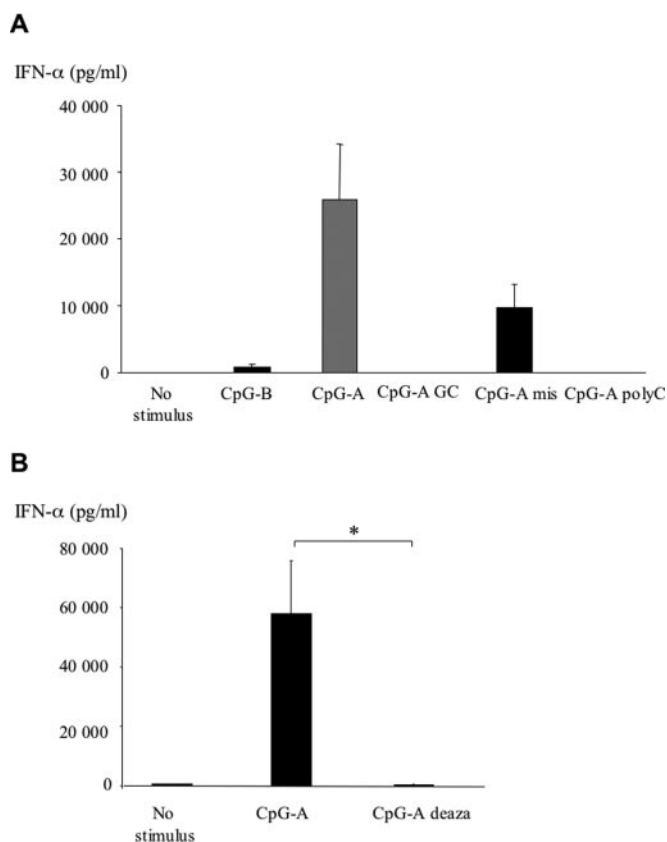


FIG. 1. G-tetrad formation is required for CpG-A-induced IFN- α production in plasmacytoid dendritic cells. PDC (5×10^4 cells/well) were incubated in the presence of CpG-B (ODN 2006), CpG-A (ODN 2216), CpG-A GC, CpG-A poly(C), CpG-A mis, or CpG-A deaza at $3 \mu\text{g/ml}$. After 48 h IFN- α was measured in the supernatants by enzyme-linked immunosorbent assay. Results are presented as means \pm S.E. of $n = 3$ (A) or $n = 8$ (B) independent experiments with different donors. *, $p < 0.05$.

significance of differences was determined by the paired two-tailed Student's t test. Differences were considered statistically significant for $p < 0.05$ (*, $p < 0.05$ and **, $p < 0.01$). Statistical analyses were performed using StatView 4.51 software (Abacus Concepts, Inc., Calabasas, CA).

RESULTS

Induction of IFN- α in Plasmacytoid Dendritic Cells by CpG-A Requires G-tetrad Formation—CpG-A is characterized by its ability to induce large amounts of IFN- α in PDC. However, the molecular basis for this feature of CpG-A is not well understood. In addition to CpG motifs that are present in both CpG-A and CpG-B, the sequence of CpG-A contains a palindrome in the center and poly(G) motifs at the 5' and the 3' end. We found that all three sequence motifs of CpG-A were required for its activity. Replacement of the CG dinucleotides to GC (CpG-A GC) completely abolished IFN- α induction in PDC (Fig. 1A). The exchange of only two bases of the palindrome motif (CpG-A mis, contains no palindrome) strongly reduced the activity of CpG-A (Fig. 1A). Replacement of the poly(G) motifs at both ends by poly(C) (CpG-A poly(C)) lead to complete loss of activity compared with CpG-A (Fig. 1A).

Poly(G) motifs within the sequence of CpG-A may contribute to the IFN- α -inducing activity by different mechanisms including enhanced uptake, immune recognition or G-tetrad formation. G-tetrad formation can be blocked by 7-deazaguanosine substitution in the poly(G) motifs (27). 7-Deazaguanosine substitution of one base in each of the poly(G) motifs of CpG-A (CpG-A deaza) abrogated the IFN- α inducing activity of CpG-A

(Fig. 1B), indicating that G-tetrad formation is required for the immunological activity of CpG-A.

Structural Analysis of CpG-A Reveals Spontaneous Multimerization of CpG-A—G-tetrads consist of at least four contiguous poly(G) motifs linked via Hoogsteen base pairing. Because one CpG-A molecule contains two poly(G) motifs, G-tetrad formation requires at least two CpG-A molecules. To analyze the extent of G-tetrad formation by CpG-A, ^{32}P -labeled ODN were analyzed on a 20% polyacrylamide gel. Under non-denaturing conditions, a high proportion of CpG-A showed a diffuse mobility pattern extending to the gel pocket indicating the formation of large and variable tertiary structures (Fig. 2A, second lane from the left). Heating of CpG-A up to 96°C for 20 min followed by rapid cooling to 4°C completely abolished the formation of tertiary structures of CpG-A (Fig. 2A, left lane); this condition also confirmed the position of the monomeric CpG-A on the gel. No tertiary structures were found for CpG-B or when the poly(G) motifs of CpG-A were replaced by poly(C) (Fig. 2A, third and fourth lanes from the left). Tertiary structures were largely diminished when the palindrome of CpG-A was destroyed by the exchange of two bases (CpG-A mis, Fig. 2A, second lane from the right). Tertiary structures were hardly detectable with a control ODN containing two poly(G) motifs at both ends but no palindrome (Tet 1.5 (28); Fig. 2A, right lane). These results indicated that CpG-A but not CpG-B has a high tendency to spontaneously form large tertiary structures and that this structure formation depends on the presence of poly(G) motifs and on the palindrome and can be broken down to the monomeric molecules by exposure to very high temperatures.

Under non-denaturing conditions the mobility of DNA on the gel is not linear to the size of the ODN. Denaturing gels disrupt Watson-Crick base pairing, thereby allowing a better estimate of the ODN length. Although large proportions of CpG-A were found to be monomeric under denaturing conditions (20 mer, Fig. 2B, left lane, indicated by 1), tertiary structures formed by CpG-A were still visible (Fig. 2B, left lane, indicated by 4 and 8). A dimer of CpG-A is expected in the area indicated by 2 (Fig. 2B, left lane). However, the first bands of higher intensity appear in higher molecular weight areas 4 and 8 (Fig. 2B, left lane) suggesting that the first stable tertiary structure is a quadruplex (4) rather than a duplex of CpG-A. Even under denaturing conditions, large tertiary structures up to the gel pocket were detected.

It has been reported that the optimal salt conditions for G-tetrad formation is a mixture of sodium and potassium, usually $\text{Na}^+:\text{K}^+$ in a 10:1 to 20:1 ratio (29). We compared spontaneous formation of tertiary structures by CpG-A under different salt concentrations (Fig. 3). CpG-A was first heated up to 96°C and then rapidly cooled on ice and incubated at 37°C or 60°C for 24 h in the presence of buffers A, B, or C. Similar formation of tertiary structures by CpG-A was seen at 37°C in all conditions tested (Fig. 3). However, tertiary structure formation was strongly reduced when CpG-A was incubated at 60°C . These results indicated that spontaneous multimerization of CpG-A occurs at physiological conditions (37°C) under both high sodium low potassium concentrations (typical for interstitial fluid) and low sodium high potassium concentrations (typical for the intracellular milieu).

Visualization of Spontaneous CpG-A Nanoparticle Formation by Atomic Force Microscopy—The presence of a large proportion of CpG-A in the very high molecular weight area and the gel pocket of the gel suggested that CpG-A may form nanometer-sized multimers. We used high resolution atomic force microscopy (AFM) for imaging of structures formed by CpG-A. This technique allows an exact measurement of the size

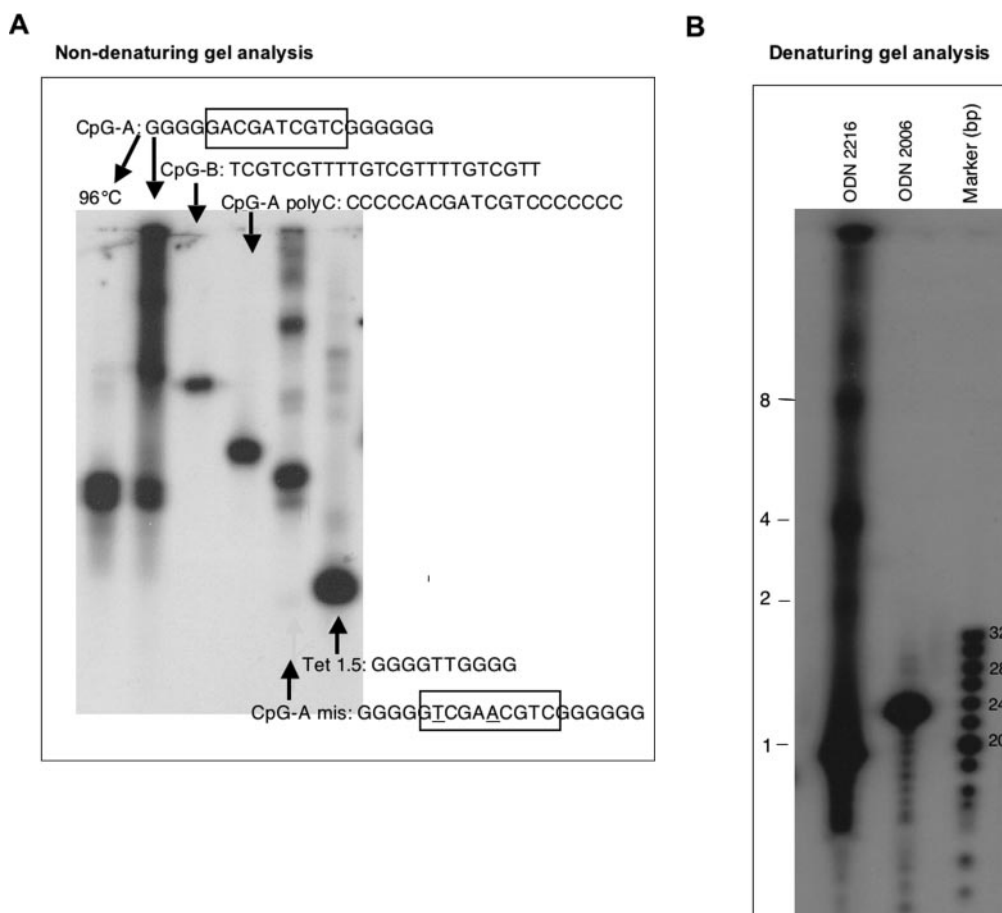


FIG. 2. **Structural analysis of CpG-A by using gel electrophoresis.** 32 P-Labeled ODN were analyzed on a 20% polyacrylamide gel. *A*, non-denaturing gel analysis of CpG-A, CpG-A poly(C), CpG-A mis, CpG-B, Tet 1.5. For the results shown by the first lane CpG-A was boiled at 96 °C for 20 min and stored on ice before gel analysis. The gel was run at a constant electric field of 8 V/cm. Palindromes are indicated by boxes; mismatched bases in the palindrome are *underscored*. *B*, denaturing gel analysis of CpG-A and CpG-B. The marker ranges from 8–32 bp. The gel was run at a constant electric field of 40 V/cm.

and the visualization of the shape of single nanometer-sized particles formed under different conditions.

For AFM imaging, CpG-A or CpG-B (6 μ g/ml) were diluted in PBS (139 mmol Na⁺/4.2 mmol K⁺, without Ca²⁺ and Mg²⁺) and deposited on mica (solid support) pretreated with 25 mM Mg²⁺Cl. AFM imaging was performed in the dynamic mode in air. We found that CpG-A forms heterogenous particles mainly composed of globular and linear structures. The maximum size of globular structures was ~50 nm; the length of linear structures exceeded 100 nm (Fig. 4). The height of structures was between 3 nm (longitudinal structures) and 10 nm (globular structures). For CpG-B no higher order structures were detectable (data not shown).

Nanoparticles Loaded with CpG-B on Their Surface Mimic the Immunological Activity of CpG-A—We hypothesized that spontaneous nanoparticle formation of CpG-A under physiological conditions may be critical for the capacity of CpG-A to induce large amounts of IFN- α in PDC. Consequently, preformed nanoparticles coated with monomeric CpG-B (unable to form higher order structures by itself) may show similar immunological activity as CpG-A. To test this hypothesis, CpG-A, CpG-B, and CpG-B GC were adsorbed to the positively charged surface of polystyrene nanoparticles. The adsorption of CpG-B to polystyrene nanoparticles (CpG-B PS) resulted in a more than 300-fold increase in IFN- α induction in PDC compared with CpG-B alone (CpG-B PS, 49,097 pg/ml *versus* CpG-B, 146 pg/ml) (Fig. 5). IFN- α induction by polystyrene-bound CpG-B was even higher than with CpG-A. The ability of CpG-A to induce IFN- α was diminished by binding to polystyrene nano-

particles. No induction of IFN- α was found with the corresponding GC control of CpG-B with (CpG-B GC PS) and without (CpG-B GC) polystyrene nanoparticles confirming that IFN- α induction in PDC is CG-dependent and that polystyrene nanoparticles have no intrinsic IFN- α inducing activity (Fig. 5A). In contrast to IFN- α production, both CpG-A and CpG-B were found equally potent to induce TNF- α in PDC. The increase of TNF- α in PDC with polystyrene nanoparticles was much lower (3-fold, Fig. 5C) as compared with the increase in IFN- α (300-fold, Fig. 5B), suggesting that the induction of TNF- α was less dependent on the presentation of CpG motifs on particles.

Internalization of Polystyrene Nanoparticles and CpG-A in Plasmacytoid Dendritic Cells—The findings of similar amounts of TNF- α induced by CpG-A and CpG-B and the relatively small increase of TNF- α induction for CpG-B when loaded on polystyrene nanoparticles (see Fig. 5) make it unlikely that simply increased uptake of the ODN in the presence of nanoparticles is responsible for the dramatic increase in IFN- α induction in PDC. To further investigate this possibility we examined internalization of fluorescently labeled ODN in PDC with and without polystyrene nanoparticles. Internalization of ODN was determined as the increase of PDC-associated fluorescence intensity at 37 °C over the background of surface binding of ODN determined at 4 °C. We found that the uptake of CpG-B with and without polystyrene nanoparticles and of CpG-A were in the same range (~2-fold increase over background within 1.5 h, Fig. 6, A and B). These data suggested that an increased uptake of ODN is not the mechanism by

**Non-denaturing gel analysis of CpG-A:
different buffers and temperatures**

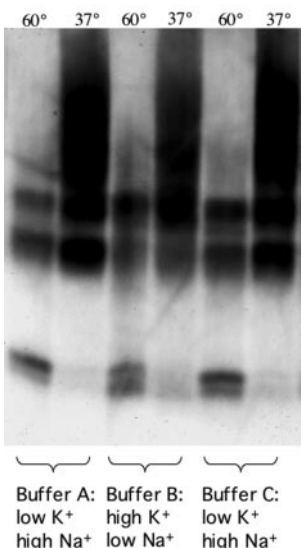


FIG. 3. Temperature-dependent formation of higher order structures by CpG-A. Digoxigenin-labeled CpG-A diluted in water was heated at 95 °C for 2 min and then immediately put on ice and mixed with four different buffers (1:1 with 2-fold concentrated buffers): A, 4 mmol K⁺, 143 mmol Na⁺; B, 155 mmol K⁺, 10 mmol Na⁺; C, 10 mmol K⁺, 150 mmol Na⁺. Samples were incubated for 24 h at 37° or 60 °C as indicated before they were analyzed on a non-denaturing 16% polyacrylamide gel at room temperature (30 min at 100 V followed by 3 h at 200 V).

**Structural analysis of CpG-A by
atomic force microscopy**

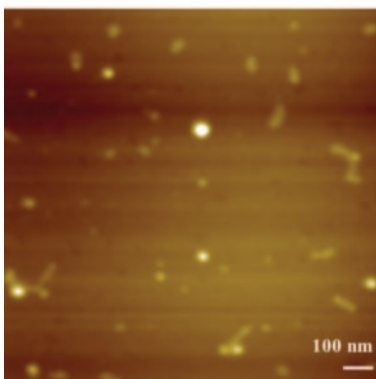


FIG. 4. Analysis of spontaneous nanoparticle formation by CpG-A by using atomic force microscopy. CpG-A (6 μg/ml) was diluted in PBS (4.2 mmol K⁺, 139 mmol Na⁺ without Ca²⁺ and Mg²⁺) and deposited on mica (solid support) pretreated with 25 mM Mg²⁺Cl⁻ dried under vacuum. Atomic force microscopy was performed in the dynamic mode in air. The scale bar is 100 nm. One representative of more than five images is shown.

which nanoparticle formation (CpG-A or CpG-B PS) contributes to the capacity of ODN to induce IFN-α in PDC.

DISCUSSION

Although type I IFN induction by viruses has been known for decades, CpG-A was the first synthetic stimulus to trigger large amounts of IFN-α in human PDC (8), whereas other CpG ODN were potent activators of PDC and B cell differentiation but not of IFN-α production. The mechanism behind the strong IFN-α inducing potency of CpG-A has remained unclear. Here we provide evidence that CpG-A spontaneously and under physiological conditions forms stable nanoparticles of a size similar to viruses (20 to 100 nm).

AFM has been used for imaging of DNA (30). In our study we used AFM to confirm the formation of higher order structures observed with polyacrylamide gel electrophoresis. AFM allows one to visualize the size and the shape of the structures formed by CpG-A. We found that CpG-A but not CpG-B forms both globular and linear structures. Linear structures (termed G-wires) but no globular structures have been observed by another group analyzing the G-tetrad formation of a poly(G) containing ODN sequence (Tet 1.5, containing poly(G) but no palindrome) found in telomers (28, 31). Under physiological conditions used in our study, Tet 1.5 was weak at forming higher order structures when compared with CpG-A.

In the literature, G-tetrad-based quadruplex formation has been demonstrated to depend on the concentration of sodium and potassium in the ODN diluent (20, 21). In a study by Basu and Wickstrom (32), no quadruplex structure formation of poly(G) containing ODN was observed at 37 °C under low sodium high potassium (intracellular), high sodium low potassium (interstitial), or physiological sodium concentrations without potassium. Some quadruplex formation in that study was only found at lower temperatures.

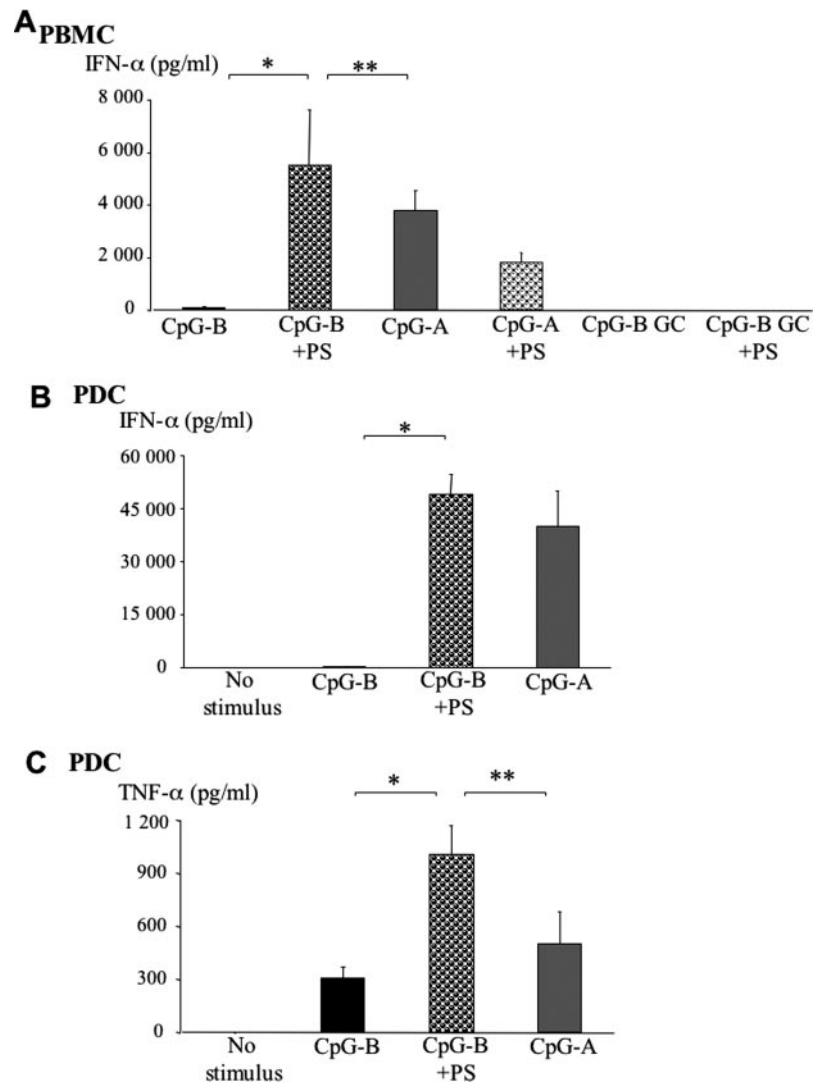
Our finding that a palindrome enables spontaneous formation of nucleic acid nanoparticles of poly(G) containing sequences under physiological conditions is novel. Spontaneous formation of higher order structures by CpG-A was seen at 37 °C and for salt concentrations typical for both the interstitial (high sodium, low potassium) or intracellular (low sodium, high potassium) milieu. According to our results the palindrome seems to catalyze G-tetrad formation of the poly(G) ends, allowing structures to be formed even under conditions that otherwise do not support G-tetrad formation.

Based on our gel and AFM analysis we propose a model in which two monomeric CpG-A oligonucleotides form a duplex via Watson-Crick base pairing of their palindrome sequences. Subsequently, four poly(G) ends of the two duplexes are linked together via G-tetrads (quadruplex, illustrated in Fig. 7). Because the formation of G-tetrads requires that four poly(G) sequences are positioned close to each other at the same time, duplex formation via palindromes largely increases the probability of such an event (increased by the square of the reciprocal value of the probability of the single event divided by two, $[1/p]^2/2$). This may explain why G-tetrad formation is facilitated by a palindrome within the oligonucleotide as observed in our study. There are two possibilities for further polymerization of quadruplexes: another duplex is linked via G-tetrad (Fig. 7B) resulting in a linear extension of the polymer, or two monomers bind to the quadruplex by Watson-Crick base pairing leading to a bifurcation (Fig. 7C). This is possible because Watson-Crick base pairing of the original dimer is weakened by neighboring Hoogsteen base pairing of the G-tetrad (Watson-Crick, 2.0 nm; Hoogsteen, 2.8 nm) (33).

This model is supported by the appearance of both globular (bifurcation required) and linear structures formed by CpG-A in the AFM image. Further support comes from the analysis of CpG-A under denaturing conditions. In denaturing gels, higher order structures of CpG-A appeared as a ladder pattern. As expected, a duplex of two CpG-A molecules was not stable. Consistent with four single strands required for a G-tetrad, the smallest complex stable on a denaturing gel was a quadruplex. Not only quadruplexes but also complexes of higher order resisted denaturing conditions, indicating that such complexes contained multiple G-tetrads. In agreement with our results, it has been reported that G-tetrad complexes once formed are resistant to denaturation (28).

It has been postulated that CpG-A might signal through a

FIG. 5. CpG-B-coated polystyrene nanoparticles mimic the immunological activity of CpG-A. Positively charged polystyrene nanoparticles (PS) were loaded with (negatively charged) CpG-B (CpG-B + PS), CpG-B GC (CpG-B GC + PS), or CpG-A (CpG-A + PS) as described under "Materials and Methods." Peripheral blood mononuclear cells (A) or PDC (B and C) were incubated with ODN-loaded on PS or with ODN alone (final concentration of ODN with and without PS was 3 $\mu\text{g}/\text{ml}$). After 48 h supernatants were collected and IFN- α (A and B) or TNF- α (C) was measured by enzyme-linked immunosorbent assay. Results are presented as means \pm S.E. of four independent experiments with different donors. *, $p < 0.05$; **, $p < 0.01$.



heteromeric or a non-TLR9 receptor (34, 35). However, several findings in our study support the concept that structure formation rather than a different receptor is responsible for the distinct properties of CpG-A as compared with CpG-B. (i) The capacity to induce IFN- α in PDC was closely linked to the ability of higher order complex formation by CpG-A. Elimination of the palindrome sequence by the exchange of two bases or replacement of poly(G) with poly(C) or introduction of one deazaguanosine substitution (inhibits G-tetrad formation) in each poly(G) motif strongly reduced both structure formation and IFN- α induction. (ii) Polystyrene nanoparticles loaded with CpG-B (lacking palindrome or G-tetrads) were equally effective as CpG-A at inducing IFN- α in PDC. (iii) IFN- α inducing activity of both CpG-A and CpG-B loaded nanoparticles was highly CpG-specific; the corresponding GC-controls were completely inactive.

A possible explanation for higher IFN- α inducing activity of CpG-A may be simply an enhanced uptake of CpG-A as compared with CpG-B. It has been proposed that the higher activity of poly(G) containing CpG oligonucleotides is caused by an increased uptake of the oligonucleotide (34, 36). Binding of poly(G) to scavenger receptors was reported to mediate enhanced internalization in myeloid cells (37, 38). Another group reported that scavenger receptor A contributes to cell surface binding of DNA but was not essential for the immunological activity of CpG ODN (39). In another study it was reported that CpG ODN-loaded cationic poly(D,L-lactide-co-glycolide) micro-

particles (cPLGA, 1.4 μm) show a high adsorption to the surface of PDC within 30 min (40). However, the actual proportion of internalized CpG ODN has not been quantified in this study. In our study with PDC, similar levels of internalization were observed for CpG-A, CpG-B, and CpG-B loaded on polystyrene nanoparticles. Furthermore, scavenger receptor A was not expressed on PDC.³ Thus, the different potency of CpG-A and CpG-B to induce IFN- α in PDC is not caused by a quantitative difference in ODN uptake. This is further supported by our observation that despite the large difference in IFN- α induction CpG-A and CpG-B induce the same level of TNF- α .

If not enhanced uptake, what other mechanisms could be responsible for higher IFN- α inducing activity of CpG-ODN when presented in a particle-like structure? One explanation might be that the dense spatial configuration of CpG motifs in particles leads to clustering and cross-linking of TLR9 in lipid rafts. The concept of TLR9 cross-linking was recently proposed by another group based on their finding that unmodified phosphodiester ODN gained immunostimulatory properties if they contain one poly(G) motif in addition to a CpG motif and that this gain of activity was associated with aggregate formation of the ODN (41). However, no palindrome was present in their phosphodiester ODN sequences, and the immunological activity (IL-12 production in murine bone marrow cells) of these

³ S. Rothenfusser, unpublished results.

A

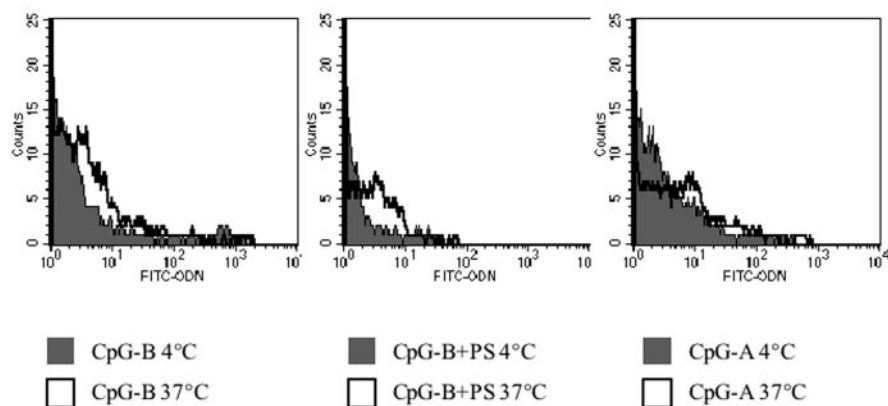
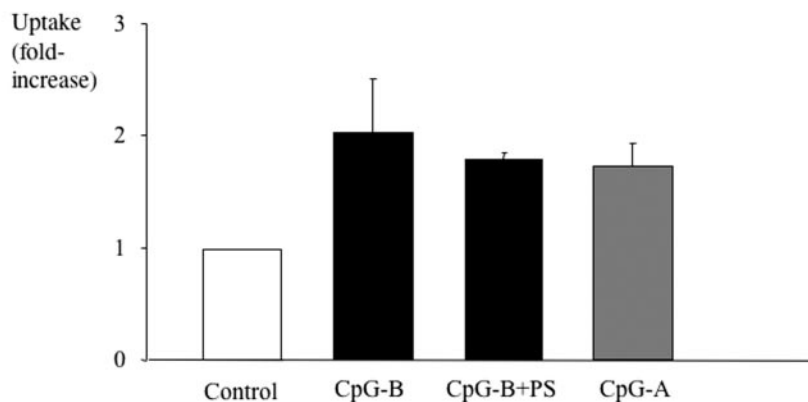


FIG. 6. Internalization of CpG-B-coated polystyrene nanoparticles and of CpG-A in plasmacytoid dendritic cells. PDC were incubated at 4 °C or at 37 °C with fluorescein-labeled CpG-B loaded on polystyrene nanoparticles (CpG-B + PS), CpG-B alone, or CpG-A. After 1.5 h PDC were washed twice and the amount of ODN associated with PDC was analyzed by using flow cytometry. *A*, histogram analysis of fluorescence intensity at 4 °C (gray) and 37 °C (white). One representative of two experiments is shown. *B*, uptake of ODN is quantified as -fold increase of the median of fluorescence intensity of samples incubated at 4 °C and at 37 °C. Means \pm S.E. of two experiments are depicted.

B



Model of higher order structures by CpG-A

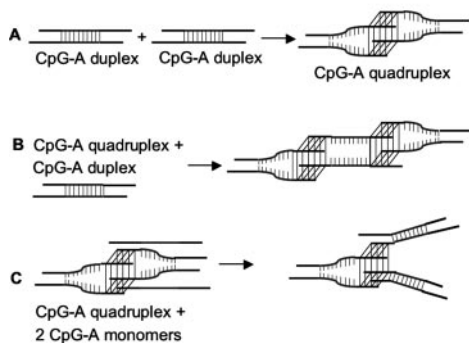


FIG. 7. Model for spontaneous nanoparticle formation by CpG-A. *A*, two CpG-A molecules form a duplex via Watson-Crick base pairing of their palindromes. Two CpG-A duplexes form a quadruplex via G-tetrad formation of four poly(G) ends. *B*, association of the quadruplex with another CpG-A duplex leads to a linear structure consisting of three duplexes linked via G-tetrads (bivalent with regard to G-tetrad formation). *C*, G-tetrad formation destabilizes the CpG-A duplexes of the quadruplex. Two other CpG-A monomers replace the original duplex by forming two new duplexes. This creates a bifurcation resulting in a structure with three ends each capable of forming another G-tetrad (trivalent with regard to G-tetrad formation). Polymerization of bivalent structures (A and B) leads to linear CpG-A multimers. Polymerization of trivalent structures (C) leads to globular CpG-A multimers (nanoparticles). Black, poly(G) sequences; gray, palindrome sequence.

ODN in their study did not even reach the potency of a standard phosphorothioate CpG-B ODN. The phosphorothioate CpG-B ODN 2006, one of the most potent CpG-B ODN known to date, in our study was by magnitudes less active than CpG-A, the ODN structurally analyzed by us.

Differences in the kinetics of IFN- α induction by CpG-A and CpG-B may contribute to the quantitative difference of IFN- α induction seen with both types of CpG ODN. In a previous study we have demonstrated that IFN- α induction by CpG-A but not CpG-B was dependent on the positive type I IFN receptor feedback loop (42). Because of processing of nucleic acid particles like CpG-A, CpG motifs will be present in the endosome of PDC for a longer period of time required to make use of the type I IFN receptor positive feedback loop.

In conclusion, our results reveal that spontaneous nucleic acid nanoparticle formation is essential for the distinct immunological activity of CpG-A to induce large amounts of IFN- α in PDC. The information on the structural potential of CpG-A as described in this work is important for the use of CpG-A as a potent synthetic stimulus for IFN- α induction *in vitro* as well as for its clinical development *in vivo*. Quality controls of CpG-A for both *in vitro* studies and for clinical application will not only have to assure the length and correct sequence of the single molecule but also need to quantify and standardize the size of the nanoparticles.

Acknowledgments—We thank Norbert Lubenow and Andreas Greinacher from the Institute of Immunology and Transfusion Medicine at the University of Greifswald, Greifswald, Germany, for providing blood products.

REFERENCES

1. Cella, M., Jarrossay, D., Facchetti, F., Alebardi, O., Nakajima, H., Lanzavecchia, A., and Colonna, M. (1999) *Nat. Med.* **5**, 919–923
2. Siegal, F. P., Kadowaki, N., Shodell, M., Fitzgerald-Bocarsly, P. A., Shah, K., Ho, S., Antonenko, S., and Liu, Y. J. (1999) *Science* **284**, 1835–1837
3. Akira, S., Takeda, K., and Kaisho, T. (2001) *Nat. Immunol.* **2**, 675–680
4. Hornung, V., Rothenfusser, S., Britsch, S., Krug, A., Jahrsdörfer, B., Giese, T., Endres, S., and Hartmann, G. (2002) *J. Immunol.* **168**, 4531–4537
5. Krug, A., Towarowski, A., Britsch, S., Rothenfusser, S., Hornung, V., Bals, R., Giese, T., Engemann, H., Endres, S., Krieg, A. M., and Hartmann, G. (2001) *Eur. J. Immunol.* **31**, 3026–3037
6. Kadowaki, N., Ho, S., Antonenko, S., Malefyt, R. W., Kastelein, R. A., Bazan, F., and Liu, Y. J. (2001) *J. Exp. Med.* **194**, 863–869
7. Hartmann, G., Weiner, G. J., and Krieg, A. M. (1999) *Proc. Natl. Acad. Sci. U. S. A.* **96**, 9305–9310
8. Krug, A., Rothenfusser, S., Hornung, V., Jahrsdörfer, B., Blackwell, S., Ballas, Z. K., Endres, S., Krieg, A. M., and Hartmann, G. (2001) *Eur. J. Immunol.* **31**, 2154–2163
9. Krieg, A. M. (2002) *Annu. Rev. Immunol.* **20**, 709–760
10. Hartmann, G., Weeratna, R. D., Ballas, Z. K., Payette, P., Blackwell, S., Suparto, I., Rasmussen, W. L., Waldschmidt, M., Sajuthi, D., Purcell, R. H., Davis, H. L., and Krieg, A. M. (2000) *J. Immunol.* **164**, 1617–1624
11. Hartmann, G., and Krieg, A. M. (2000) *J. Immunol.* **164**, 944–953
12. Poeck, H., Wagner, M., Battiany, J., Rothenfusser, S., Wellisch, D., Hornung, V., Jahrsdörfer, B., Giese, T., Endres, S., and Hartmann, G. (2004) *Blood* **103**, 3058–3064
13. Hartmann, G., Battiany, J., Poeck, H., Wagner, M., Kerkmann, M., Lubenow, N., Rothenfusser, S., and Endres, S. (2003) *Eur. J. Immunol.* **33**, 1633–1641
14. Marshall, J. D., Fearon, K., Abbate, C., Subramanian, S., Yee, P., Gregorio, J., Coffman, R. L., and Van Nest, G. (2003) *J. Leukocyte Biol.* **73**, 781–792
15. Vollmer, J., Weeratna, R., Payette, P., Jurk, M., Schetter, C., Laucht, M., Wader, T., Tluk, S., Liu, M., Davis, H. L., and Krieg, A. M. (2004) *Eur. J. Immunol.* **34**, 251–262
16. Hemmi, H., Kaisho, T., Takeuchi, O., Sato, S., Sanjo, H., Hoshino, K., Horiuchi, T., Tomizawa, H., Takeda, K., and Akira, S. (2002) *Nat. Immunol.* **3**, 196–200
17. Williamson, J. R., Raghuraman, M. K., and Cech, T. R. (1989) *Cell* **59**, 871–880
18. Sen, D., and Gilbert, W. (1988) *Nature* **334**, 364–366
19. Keniry, M. A. (2000) *Biopolymers* **56**, 123–146
20. Hardin, C. C., Henderson, E., Watson, T., and Prosser, J. K. (1991) *Biochemistry* **30**, 4460–4472
21. Marathias, V. M., and Bolton, P. H. (1999) *Biochemistry* **38**, 4355–4364
22. Sen, D., and Gilbert, W. (1992) *Methods Enzymol.* **211**, 191–199
23. Balagurumorthy, P., and Brahmachari, S. K. (1994) *J. Biol. Chem.* **269**, 21858–21869
24. Costa, L. T., Kerkmann, M., Hartmann, G., Endres, S., Bisch, P. M., Heckl, W. M., and Thalhammer, S. (2004) *Biochem. Biophys. Res. Commun.* **313**, 1065–1072
25. Rothenfusser, S., Hornung, V., Ayyoub, M., Britsch, S., Towarowski, A., Krug, A., Sarris, A., Lubenow, N., Speiser, D., Endres, S., and Hartmann, G. (2004) *Blood* **103**, 2162–2169
26. Fritz, H., Maier, M., and Bayer, E. (1997) *J. Colloid Interface Sci.* **195**, 272–288
27. Benimetskaya, L., Berton, M., Kolbanovsky, A., Benimetsky, S., and Stein, C. A. (1997) *Nucleic Acids Res.* **25**, 2648–2656
28. Marsh, T. C., and Henderson, E. (1994) *Biochemistry* **33**, 10718–10724
29. Sen, D., and Gilbert, W. (1990) *Nature* **344**, 410–414
30. Hansma, H. G., Revenko, I., Kim, K., and Laney, D. E. (1996) *Nucleic Acids Res.* **24**, 713–720
31. Marsh, T. C., Vesenska, J., and Henderson, E. (1995) *Nucleic Acids Res.* **23**, 696–700
32. Basu, S., and Wickstrom, E. (1997) *Nucleic Acids Res.* **25**, 1327–1332
33. Laughlan, G., Murchie, A. I., Norman, D. G., Moore, M. H., Moody, P. C., Lilley, D. M., and Luisi, B. (1994) *Science* **265**, 520–524
34. Gursel, M., Verthelyi, D., Gursel, I., Ishii, K. J., and Klinman, D. M. (2002) *J. Leukocyte Biol.* **71**, 813–820
35. Verthelyi, D., Kenney, R. T., Seder, R. A., Gam, A. A., Friedag, B., and Klinman, D. M. (2002) *J. Immunol.* **168**, 1659–1663
36. Dalpke, A. H., Zimmermann, S., Albrecht, I., and Heeg, K. (2002) *Immunology* **106**, 102–112
37. Kimura, Y., Sonehara, K., Kuramoto, E., Makino, T., Yamamoto, S., Yamamoto, T., Kataoka, T., and Tokunaga, T. (1994) *J. Biochem. (Tokyo)* **116**, 991–994
38. Lee, S. W., Song, M. K., Baek, K. H., Park, Y., Kim, J. K., Lee, C. H., Cheong, H. K., Cheong, C., and Sung, Y. C. (2000) *J. Immunol.* **165**, 3631–3639
39. Zhu, F. G., Reich, C. F., and Pisetsky, D. S. (2001) *Immunology* **103**, 226–234
40. Fearon, K., Marshall, J. D., Abbate, C., Subramanian, S., Yee, P., Gregorio, J., Teshima, G., Ott, G., Tuck, S., Van Nest, G., and Coffman, R. L. (2003) *Eur. J. Immunol.* **33**, 2114–2122
41. Wu, C. C., Lee, J., Raz, E., Corr, M., and Carson, D. A. (2004) *J. Biol. Chem.* **279**, 33071–33078
42. Kerkmann, M., Rothenfusser, S., Hornung, V., Towarowski, A., Wagner, M., Sarris, A., Giese, T., Endres, S., and Hartmann, G. (2003) *J. Immunol.* **170**, 4465–4474